# Understanding the Binding of 5-Substituted 2′-Deoxyuridine Substrates to Thymidine Kinase of Herpes Simplex Virus Type-1

Hans De Winter and Piet Herdewijn*

*Laboratory of Medicinal Chemistry, Rega Institute for Medical Research, Katholieke Universiteit Leuven, Minderbroedersstraat 10, B-3000 Leuven, Belgium*

*Received April 10, 1996*[⊗]

Thymidine kinase from HSV-1 (HSV-1 TK) is a key enzyme in the metabolic activation of antiviral nucleosides. High affinity of such compounds for the enzyme is required for efficient phosphorylation. In this study, affinity data from a series of 5-substituted 2′-deoxyuridine substrates in combination with the crystal structure of the viral enzyme were used to investigate the structural factors influencing the affinity of these compounds for the enzyme. Calculations showed that the binding energetics and conformations of thymidine and the 5-substituted 2′-uridine analogues are similar. The major part of the binding energy arises from interactions involving sugar and base moieties. Small differences in affinity for the enzyme are explained by the hydrophobicity of the 5-substituent or by its energetic complementarity with the active site pocket. In designing high-affinity nucleoside substrates of HSV-1 TK, care should be taken to maintain the geometry of the base moiety and sugar hydroxyl functionalities. Substitutions at the 5-position of the nucleobase should be lipophilic and characterized by well-defined geometrical properties. The present study represents a first quantitative explanation for HSV-1 TK affinity of 5-substituted 2′-deoxyuridines which are historically the first group of selective antivirals. The results may be used to design new and more potent compounds.

## Introduction

Herpes simplex virus (HSV) establishes latent infections in human nerve tissue and exists as type-1 (HSV-1) and type-2 (HSV-2). Infections of HSV-1 in humans can lead to acute gingivostomatitis, herpes labialis, or ocular disease, while HSV-2 accounts for most cases of herpes genitalis.

Antiviral chemotherapy started with the discovery in 1959 of the antiherpes activity of 5-iodo-2′-deoxyuridine by serendipity.[1] The structure of 5-iodo-2′-deoxyuridine is very similar to that of thymidine, *i.e.* the replacement of the methyl group in the 5-position of the uracil moiety by a iodine. This small difference, however, is sufficient to render 5-iodo-2′-deoxyuridine a selective antiviral compound. This landmark in antiviral chemotherapy was later followed by others; the most important are the discovery of acyclovir as a nontoxic antiherpes agent and the discovery of 3′-azido-3′-deoxythymidine as the first approved anti-HIV nucleoside. The resemblance of this latter molecule with the structure of thymidine is also striking. Here the 3-hydroxyl group of the deoxyribose moiety is replaced by an azido group. Both compounds (5-iodo-2′-deoxyuridine and 3′-azido-3′-deoxythymidine) also demonstrate a very similar mode of action. They have to be phosphorylated to their corresponding triphosphate, and in this form they selectively interact with viral enzymes (DNA polymerase and reverse transcriptase, respectively). Although the structure of 5-iodo-2′-deoxyuridine and its mode of action have been known for over 30 years, the way it interacts with its metabolic and target enzymes still remains puzzling.

The discovery of 5-iodo-2′-deoxyuridine as a selective HSV-1 drug has led to the synthesis of an overwhelming number of other 5-substituted 2′-deoxyuridine compounds (for a review, see ref 2), of which the best known is (*E*)-5-(bromovinyl)-2′-deoxyuridine.[3] Structure−activity studies of this class of compounds have only been descriptive until now after the recent discovery of a new series of 5-heteroaromatic-substituted 2′-deoxyuridines and the availability of the crystal structure of herpes simplex type-1 thymidine kinase.

The genome of HSV-1 encodes several virus specific enzymes involved in nucleoside metabolism, one of them being thymidine kinase (TK). This enzyme phosphorylates thymidine to its corresponding 5'-monophosphate, using ATP as its phosphoryl source. Therefore, TK is a crucial enzyme in the salvage pathway of thymidine-5'-triphosphate, which is the precursor of the thymidine incorporated in DNA. Viral TKs differ in many aspects from human TK and are therefore important targets for chemotherapy. The viral enzymes have much broader substrate specificity than the corresponding human enzyme, which only recognizes thymidine as a substrate while the viral enzymes even accept L-thymidine, guanine nucleosides, carbocyclic nucleosides, and many 5-substituted 2′-deoxyuridine analogues.[4]

HSV-1 TK is not essential for viral replication in cell culture, but it is an important enzyme for the pathogenicity of the virus.[5,6] However, also significant for the design of antiviral compounds is that HSV-1 TK is a key enzyme in the metabolic activation of modified nucleosides as antiviral agents. The general mode of action of these types of antiviral agents is that they are phosphorylated to their 5′-monophosphates by HSV-1 TK. The modified nucleosides have a much higher affinity for HSV-1 TK than for the cellular enzyme, and therefore preferential phosphorylation occurs mainly in virus-infected cells. The 5′-monophosphates are then further phosphorylated to their 5′-triphosphates by several other cellular kinases, and these triphosphates can either act as competitive inhibitors to TTP of the viral DNA polymerase or function as substrates for this enzyme and become incorporated into the viral DNA.

[⊗] Abstract published in *Advance ACS Abstracts,* October 15, 1996.

S0022-2623(96)00278-6 CCC: $12.00 

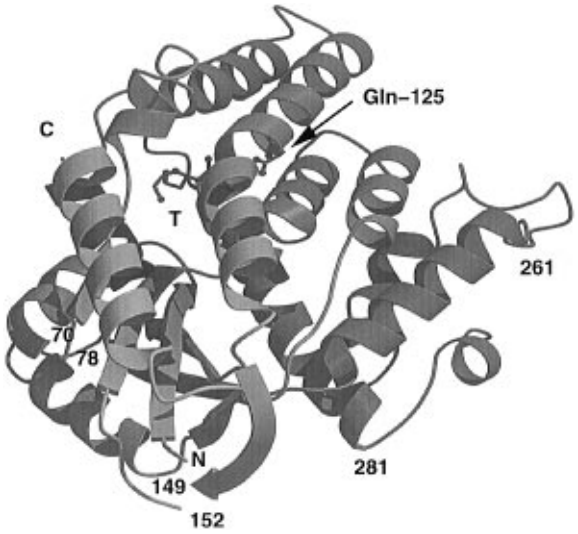


**Figure 1.** An outline of HSV-1 thymidine kinase. Thymidine (T) and Gln-125 emphasize the location of the active site pocket. Loops between residues 149−152, 70−78, and 261−281 are missing from the crystal structure. The C- and N-termini are labeled C and N, respectively.

Thymidine kinase, whose crystal structure has recently been solved at 2.8 and 2.2 Å resolution for the complexes with thymidine and ganciclovir, respectively,[7] is the first enzyme involved in the metabolic activation of antiviral nucleosides. Therefore, it might be advantageous for an effective anti-HSV-1 nucleoside to show high affinity for the viral thymidine kinase. Thus, any project which targets the design of modified nucleosides as anti-HSV compounds should incorporate some estimates on the rate of phosphorylation of the designed nucleosides by viral TK, and hence should develop an understanding about the interaction of HSV-1 TK with its substrates at the molecular level.

In the present work, computer simulations were used to investigate these interactions and to examine structural features important for 5-substituted 2′-deoxyuridine substrate recognition by HSV-1 TK. This series of 5-substituted nucleosides, recently discovered by our group, are selectively phosphorylated by HSV-1 TK.[8−10] Their affinity for the enzyme, expressed in terms of $IC_{50}$ values measured against the natural substrate, ranges from 2 to 150 $\mu$M, depending on the substitution pattern at the 5-position. These compounds differ from the natural substrate thymidine only by a different substitution at the 5-position and provide, therefore, an interesting tool for the analysis of the nature of molecular recognition between HSV-1 TK and 5-substituted 2′-deoxyuridine analogues. It is expected that the results of this study may be of potential interest to drug designers and chemists in their search for improved HSV-1 antivirals. Moreover, this study gives a theoretical basis for an historical discovery in antiviral chemotherapy.

## The Players

**The Crystal Structure of HSV-1 TK.** HSV-1 TK has been crystallized in complex with either thymidine or ganciclovir.[7] The molecule consists of an ab structure made up of 13 α-helices, two $3_{10}$-helices, and seven $\beta$-sheets (Figure 1). The five-stranded $\beta$-sheet forms part of the core of the molecule, which contains the active site. Although the sugar equivalents of both ligands exhibit similar binding arrangements in the active-site pocket, comparison of the nucleobase of ganciclovir with that of thymidine shows that the guanine base is flipped by approximately 180°, so that its O6 atom is located in a pocket on the opposite side of the 5-methyl group of thymidine (Figure 2). As a result of these different binding modes, and because of the high structural resemblance between thymidine and the substrates used for this study, we have taken the crystal structure of the thymidine−TK complex as the starting point for all modeling experiments. It should be noted that, apart from the amide function of Gln-125 which is rotated by 180°, no other remarkable differences between the two structures in the orientations of the residues lining the pocket are observed (Figure 2).

The crystal structure of HSV-1 TK does not contain an ATP molecule. Instead, a sulfate ion is observed at the putative position of the $\beta$-phosphate of ATP.[7] This sulfate-binding site is located in close proximity to the 5′-hydroxyl function of thymidine (S···O5′ distance is 6.5 Å) and is coordinated by the side chains of Arg-222, Arg-163, Gln-221, and by the main-chain NH functions of Gly-59, Met-60, Gly-61, Lys-62, and Thr-63.[7]

**The Substrates.** The 5-substituted 2′-deoxyuridine substrates which have been used for the computational analysis, together with their affinities for the HSV-1 TK enzyme described in the literature,[8−10] are listed in Figure 3. Basically, the structures can be divided into two classes.

The first group involves 5-(thien-2-yl)-2′-deoxyuridine (**1**) as lead compound, with an $IC_{50}$ value around 2 $\mu$M. Affinity for the enzyme is retained when the heterocyclic ring is connected *via* its 3-position (**8**), when the ring is replaced by an isothiazole (**7**), or when a halogen or methyl group is introduced at the 5-position of the 5-(thien-2-yl) ring (**2**, **5**, and **6**). In contrast, halogen substitutions at the 3-position of the thien-2-yl ring and the 4-position of the thien-3-yl ring decrease the affinity by approximately 1 order of magnitude (**3**, **4**, and **9**).

The second group includes 5-(furan-2-yl)-2′-deoxyuridine (**10**) as lead structure. As in the case of the thiophene compounds, affinity is retained when the furan ring is connected *via* its 3-position (**13**). However, in contrast to the thiophene derivatives, affinity decreases significantly when a halogen group is substituted at the 5-position of the furan-2-yl ring (**11** and **12**) or when the heterocyclic ring is replaced by an isoxazole (**14** and **15**).

Clearly, there is a difference between both classes of molecules. Crystal structure analysis revealed that all compounds have a quasi-coplanar geometry between the five-membered heterocyclic ring and the uracil base (Figure 4).[11−14] Intramolecular interactions stabilize this coplanarity. Interestingly, in the 2-thienyl series of compounds, coplanarity is stabilized by an interaction between the O4 carbonyl group of the uracil base and the sulfur atom of the thiophene ring (Figure 4, structure **A**). A similar orientation for the isothiazole derivative (Figure 4, structure **B**) has been deduced from its NMR spectrum[15] and quantum-chemical calculations, which predict a stability of 17 kJ/mol of the NMR observed orientation relative to the other possibility.[15] In contrast, the orientations of the 2-furanyl and isoxazolyl rings are clearly different from the thiophene

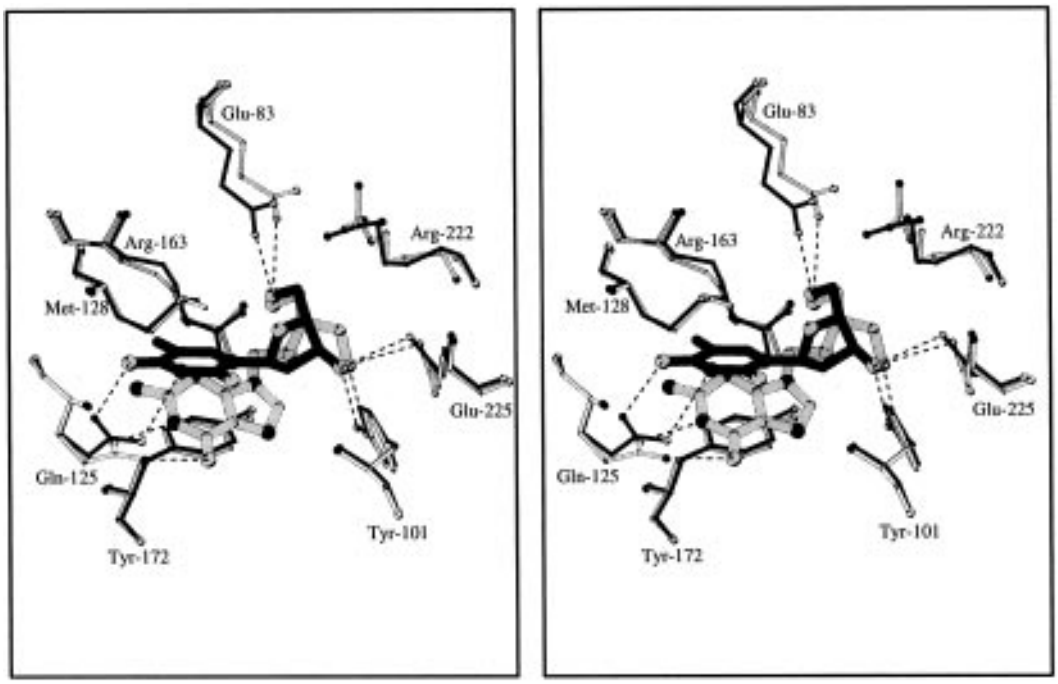


**Figure 2.** Stereoview comparing the binding modes of thymidine (dark gray bonds) and ganciclovir (light gray bonds) in the active site pocket of HSV-1 TK. Oxygen and nitrogen atoms are drawn as light and dark gray spheres, respectively. Hydrogen bonds are indicated as dashed lines. There is a remarkable overlap between the amino acid side chains in the two active-site pockets. The only exception is Gln-125, whose amide functionality is flipped approximately 180° between the two crystal forms in order to optimize hydrogen-bonding opportunities.

analogues, as they are stabilized by intramolecular interactions between the oxygen of the heterocycles and the H6 atom of the uracil base (Figures 4, structures **C** and **D**). The oxygens of the furanyl and isoxazolyl rings point therefore in an opposite direction compared to the sulfur atoms of the thienyl or isothiazolyl rings. The structures of the 3-thienyl and 3-furfuryl compounds are stabilized by an intramolecular contact between O4 of the uracil base and H2 of the heteroaromatic rings (Figure 4, structure **E**), which is analogous with the stabilizing O4···Hα interaction observed in the crystal structure of (*E*)-5-(bromovinyl)-2′-deoxyuridine (Figure 4, structure **F**).[16] Care was taken to maintain these specific conformations during the docking and energy minimization calculations by the use of appropriate torsion angle potentials.

The high structural similarity between the 17 5-substituted 2′-deoxyuridine analogues suggests that the loss of entropy upon binding the enzyme may be similar for all compounds. The 5-substituted uracil bases are planar, conjugated, and rigid systems, making them ideally suited for structure−affinity studies such as these.

## Results

**Binding of Thymidine. (A) Active Site Interactions.** A stereoplot of the crystal structure with thymidine in the active site of HSV-1 TK is shown in Figure 2.[7] Three hydrogen bonds, involving the 3′- and 5′-hydroxyl groups of thymidine, link the sugar moiety of thymidine with the enzyme, while the nucleobase forms two hydrogen bonds through atoms N3 and O4. In addition to these hydrogen bond interactions, the uracil base is sandwiched or stacked between the ϵ-methyl group of Met-128 on one side and the aromatic side chain of Tyr-172 along the other side. The 5-methyl group is located in a small hydrophobic pocket lined by residues of Tyr-132, Ala-167, Ala-168 (not shown), and the aliphatic side chain of Arg-163.

**(B) Binding Energetics.** A decomposition of the total binding energy of the minimized thymidine−HSV-1 TK complex on a per-residue basis or separated into individual contributions for the base and sugar part is listed in Table 1. Although the results are slightly dependent on the applied dielectric for calculating the interaction energies, the main conclusions remain the same. More than 80% of the total interaction energy comes from the interaction with only six residues, namely the four hydrogen bond partners Glu-83, Glu-225, Gln-125, Tyr-101, and residues Tyr-172 and Met-128, which sandwich the nucleoside base by means of stacking interactions. Thus, the major binding forces between thymidine and enzyme arise from hydrogen-bonding interactions involving the two hydroxyl groups on the sugar moiety and the amide function of the nucleobase, together with stacking interactions of the base plane. These conclusions are consistent with the decreased affinity of either ganciclovir ($IC_{50} = 50\ \mu M$),[17] where the purine base is less well stacked compared to thymidine, or acyclovir ($IC_{50} > 500\ \mu M$),[17] where only one hydroxyl function is available for hydrogen-bonding interactions.

**Binding of 5-Substituted-2′-Deoxyuridine Substrates. (A) Exploration of Alternative Binding Modes for These Compounds.** Considering the structural resemblance between the 5-substituted 2′-deoxyuridine analogues and thymidine, a binding conformation similar to the binding mode of thymidine seems reasonable at first sight. However, in principle, eight different binding modes are possible on paper, and these are shown in Figure 5.

The eight possible binding complexes are distinguished either by the side-chain conformation of Gln-125 (Table 2; compare binding modes **1a**, **1s**, **2a**, **2s** with

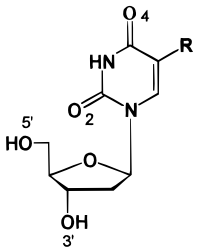

| | -R | $IC_{50}$ ($\mu$M) | | -R | $IC_{50}$ ($\mu$M) |
|---|---|---|---|---|---|
| T | —Me | 1.0 | 9 |  | 143 |
| 1 |  | 2.4 | 10 |  | 2.9 |
| 2 |  | 3.5 | 11 |  | 51 |
| 3 |  | 62 | 12 |  | 28 |
| 4 |  | 61 | 13 |  | 1.5 |
| 5 |  | 2.3 | 14 |  | 36 |
| 6 | 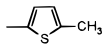 | 2.3 | 15 |  | 34 |
| 7 |  | 3.1 | 16 |  | 102 |
| 8 |  | 4.0 | 17 |  | 0.3 |

**Figure 3.** The compounds with their numbering label and experimental affinity for HSV-1 thymidine kinase. Affinity data were obtained from literature[8−10] and are the concentrations required to inhibit thymidine phosphorylation by 50% against radiolabeled thymidine used at a concentration of 1 $\mu$M. All affinities were measured under the same conditions, and highly similar $K_M$ values (0.25 $\mu$M) were found in all cases.[18]

**3a**, **3s**, **4a**, **4s**), by the orientation of the base with respect to sugar (*syn*/*anti* conformation; **1a**, **2a**, **3a**, **4a** *versus* **1s**, **2s**, **3s**, **4s**), and by the hydrogen-bonding pattern between the substrate base and the amide function of Gln-125 (**1a**, **1s**, **3a**, **3s** *vs* **2a**, **2s**, **4a**, **4s**).

However, although in principle eight different ways are feasible to dock 5-substituted substrates in the active site of HSV-1 TK, it is obvious that only a small fraction of these, if not only one, will be energetically feasible and will represent the "true" binding mode. Furthermore, since it has been shown that the 5′-hydroxyl functions of these substrates are phosphorylated to the same extent and in a similar way as the corresponding hydroxyl function of thymidine,[18] the true binding conformation will likely have its 5′-hydroxyl function in a similar orientation as found in the crystal structure of the thymidine (and ganciclovir) complex.[7]

In order to elucidate the most likely binding conformation from all the eight possibilities, we have docked and energy minimized model compound 5-(thien-2-yl)-2′-deoxyuridine (**1**) in the active site of HSV-1 TK and have subsequently evaluated each of the eight possible binding modes based on four criteria: (1) the number of hydrogen bonds between substrate and enzyme, (2)

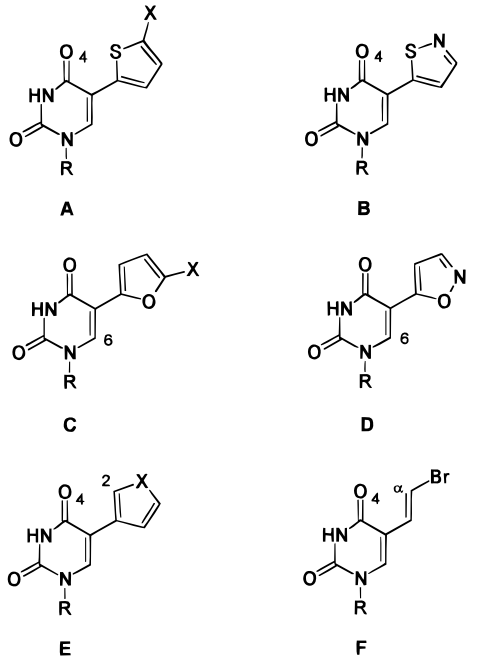

**Figure 4.** The crystal structure conformations of several 5-substituted 2′-deoxyuridine derivatives.

the root-mean-squared (rms) deviation of all active-site residues from the corresponding minimized TK-thymidine positions, (3) the distance between sugar O5′ and sulfate S atoms, and (4) the interaction energy between substrate and enzyme. The results are summarized in Table 3. Minimized binding conformations **1a**, **2a**, **3a**, and **4a** of substrate **1** in the active site of HSV-1 TK are shown in Figure 6.

Following Table 3, we believe that the most likely or true binding conformation resembles binding mode **1a** for the following four reasons. First, in binding conformation **1a** we find that the distance between the sugar O5′ and sulfate S is closer than the corresponding distance to O3′. In fact, this is observed in all cases where an *anti*-orientation between base and sugar is adopted (Table 3, binding modes **1a**, **2a**, **3a**, **4a**). If the sulfate ion is indeed located near the putative binding site of the $\beta$-phosphate of ATP,[7] we might expect from these geometries that it is atom O5′ instead of atom O3′ which will get phosphorylated by the enzyme. This is in agreement with experiment.[18] On the contrary, exactly the opposite is found for the *syn*-oriented binding conformations (**1s**, **2s**, **3s**, **4s**), where phosphorylation of the O3′ atom is expected and therefore deviates from experiment[18] (Table 3).

Second, binding mode **1a** allows the formation of the maximum number of hydrogen bonds between substrate and enzyme, leading to a much tighter substrate binding compared to the other possibilities (Figure 6). For example, due to the different orientation of the substrate in binding modes **2a** and **3a** compared to **1a** and **4a**, hydrogen-bonding opportunities of the sugar O5′ atom with Glu-83 and the sugar O3′ with Glu-225 and Tyr-101 are lost in **2a** and **3a**. In conformation **2a** this loss is partially compensated by the formation of a new hydrogen bond between O3′ and Glu-83 (Figure 6). Additionally, while the docked conformation of **4a** prior to minimization was such that it allowed for the formation of two hydrogen bonds between the substrate base and Gln-125 (Figure 5), minimization however

**Table 1.** Decomposition of the Total Binding Energy for Thymidine and 5-(Thien-2-yl)-2′-deoxyuridine (**1**)[a]

| | relative contribution to the total interaction energy (in %)[a] | | | |
|---|---|---|---|---|
| | thymidine | | 5-(thien-2-yl)-2′-deoxyuridine | |
| | $\epsilon = r$ | $\epsilon = 1$ | $\epsilon = r$ | $\epsilon = 1$ |
| Residues within 5 Å of Substrate | | | | |
| Glu-83 | −19 | −28 | −26 | −28 |
| Glu-225 | −18 | −20 | −18 | −18 |
| Gln-125 | −17 | −15 | −14 | −13 |
| Tyr-172 | −11 | −13 | −13 | −13 |
| Tyr-101 | −10 | −10 | −8 | −8 |
| Met-128 | −6 | −6 | −5 | −5 |
| Trp-88 | −4 | −3 | −6 | −5 |
| Arg-163 | −4 | 5 | 3 | 2 |
| His-58 | −3 | −4 | −5 | −4 |
| Ile-100 | −2 | −2 | −2 | −2 |
| Ile-97 | −2 | −1 | −1 | −1 |
| Ala-168 | −2 | −1 | −1 | −1 |
| Ala-167 | −1 | −2 | −4 | −4 |
| Tyr-132 | −1 | −1 | −4 | −4 |
| Gln-221 | 0 | 1 | 2 | 1 |
| Gly-129 | 0 | 0 | 0 | 0 |
| His-164 | 0 | 0 | 0 | 0 |
| Pro-165 | 0 | 0 | 1 | 0 |
| Arg-222 | 4 | 12 | 11 | 10 |
| Substrate | | | | |
| sugar moiety | −55 | −53 | −48 | −45 |
| base moiety | −40 | −42 | −35 | −36 |
| 5-substituted group | −5 | −5 | −17 | −19 |

[a] All residues within 8 Å of the substrate and the substrate itself were allowed to relax. The remaining residues were kept constrained to their crystal structure coordinates using a harmonic force constant of 1000 kJ/mol·Å$^2$. Nonbonded interactions were calculated using a 10 Å cutoff distance. Either a distance-dependent ($\epsilon = r$) or a constant dielectric ($\epsilon = 1$) was used for the calculation of electrostatic interactions. [b] The relative contribution to the total interaction energy for each residue is the interaction energy between the particular residue and the whole substrate, divided by the total interaction energy between all residues and whole substrate. The relative contribution to the total interaction energy for each substrate moiety is the interaction energy between the particular substrate moiety and the whole enzyme, divided by the total interaction energy between the whole substrate and the whole enzyme.

disrupts the hydrogen bond between the N$\epsilon$2 atom of Gln-125 and the base O2 atom, as there is a tendency for this residue to flip back to its position as found in the crystal structure with thymidine (Figure 6).

Third, taking the natural substrate thymine as a reference, the least distortion is introduced in the residues lining the pocket when substrate is docked in a conformation resembling that of **1a**. This is evident from the rms deviation between the minimized TK−**1** and TK−thymidine complexes, calculated for all residues lining the active site pocket (Table 3). In contrast, the binding of 5-substituted 2′-deoxyuridine substrates in a conformation resembling binding modes **2a** or **3a** introduces several steric clashes with, for example, Tyr-101 (binding mode **2a**) and Arg-163 (binding modes **2a** and **3a**) (Figure 6).

Fourth, the interaction energy between substrate and enzyme is significantly more favorable when the substrate is docked in binding conformation **1a** compared to the other possibilities. This is likely the consequence of a more optimal complementarity (both steric and electrostatic) between enzyme and substrate when docked in this conformation. In the case of thymidine, more than 80% of the total interaction energy arises due to interactions of the sugar hydroxyl groups hydrogen bonded to Glu-83, Glu-225, and Tyr-101, and from the

**With Gln-125 in a conformation similar as in the thymidine complex:-**

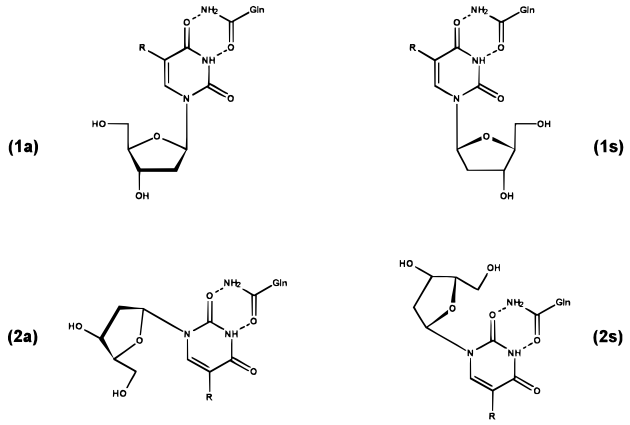


**With Gln-125 in a conformation similar as in the ganciclovir complex:-**

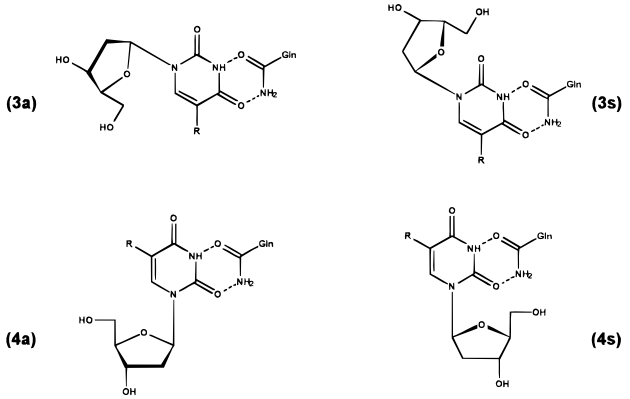


**Figure 5.** Eight possible binding orientations to dock a 5-substituted 2′-deoxyuridine substrate in the active site of HSV-1 TK. All orientations are drawn relative to the same fixed reference frame, *i.e.* the orientation of the active-site pocket is assumed to be similar in all eight cases. For a definition of -R, see Figure 3.

**Table 2.** Classification of the Possible Binding Conformations of the 5-Substituted 2′-Deoxyuridine Substrates by the Adopted Orientation of the Gln-125 Side Chain[a]

| | binding mode | |
|---|---|---|
| | 1a, 1s, 2a, 2s | 3a, 3s, 4a, 4s |
| C−C$\alpha$−C$\beta$−C$\gamma$ | 162 | −176 |
| C$\alpha$−C$\beta$−C$\gamma$−C$\delta$ | −56 | −56 |
| C$\beta$−C$\gamma$−C$\delta$−N$\epsilon$2 | −41 (resembling the values in the thymidine complex) | 130 (resembling the values in the ganciclovir complex) |

[a] Listed are the approximate starting values for the torsion angles of Gln-125 prior to energy minimization calculations (values in degrees).

pyrimidine base which is stacked between Met-128 and Tyr-172, and hydrogen bonded to Gln-125 (Table 1). It is therefore no surprise that an alternative binding arrangement lacking one of these interactions may result in a significantly decreased interaction energy, and hence, affinity.

**(B) Binding Energetics of a Typical 5-Substituted Nucleoside: 5-(Thien-2-yl)-2′-deoxyuridine (1).** A decomposition of the total binding energy for 5-(thien-2-yl)-2′-deoxyuridine (**1**) in binding conformation **1a** is

**Table 3.** Description of the Eight Possible Binding Conformations of 5-(Thien-2-yl)-2′-deoxyuridine (**1**) in the Active Site of HSV-1 TK[a]

| binding mode | *syn*/*anti*[b] | HB[c] | rms[d] | *d*(O5′···S)[e] | *d*(O3′···S)[f] | interaction energy[g] $\epsilon = 1$ | interaction energy[g] $\epsilon = r$ |
|---|---|---|---|---|---|---|---|
| **1a** | anti | 5 | 0.4 | 7.0 | 8.8 | −316 | −311 |
| **1s** | syn | 3 | 0.7 | 12.0 | 7.8 | −259 | −250 |
| **2a** | anti | 3 | 1.1 | 7.6 | 8.0 | −228 | −187 |
| **2s** | syn | 3 | 0.9 | 11.2 | 7.8 | −224 | −213 |
| **3a** | anti | 2 | 0.8 | 9.1 | 11.8 | −244 | −234 |
| **3s** | syn | 1 | 0.8 | 11.8 | 8.1 | −255 | −211 |
| **4a** | anti | 4 | 0.5 | 6.6 | 8.7 | −292 | −297 |
| **4s** | syn | 3 | 0.5 | 11.8 | 7.8 | −242 | −239 |

[a] Described in terms of the number of hydrogen bonds between substrate and enzyme, the rms deviation of all active-site residues from their corresponding minimized TK−thymidine positions, the distance between sugar O5′ and O3′ atoms and sulfate S atoms, and the interaction energy. Each binding conformation was generated by manually docking substrate **1** in the required orientation, followed by energy minimization until the gradient dropped below 0.01 kJ/mol·Å. A nonbonded cutoff of 10 Å in conjunction with a dielectric constant of $\epsilon = 1$ or $\epsilon = r$ was used. All residues within 8 Å of the substrate and the substrate itself were allowed to relax. The remaining residues were kept constrained to their crystal structure positions using a harmonic force constant of 1000 kJ/mol·Å$^2$. The reported number of hydrogen bonds (HB), rms deviation (rms), and distances between substrate hydroxyls and sulfate S [*d*(O5′···S) and *d*(O3′···S)] are from the minimized complexes calculated with a distance-dependent dielectric $\epsilon = r$. Similar results were obtained using a constant dielectric $\epsilon = 1$ but are not shown for clarity. [b] The orientation of the substrate base moiety with respect to its sugar moiety. In the *syn* orientation, the base oxygen O2 is positioned above the sugar ring, while O2 is oriented away from the sugar ring in the *anti* conformation. [c] Number of hydrogen bonds between substrate and enzyme in the minimized complex. The definition of a hydrogen bond was solely based on distance criteria, *i.e.* the actual distance between the non-hydrogen atoms had to be smaller than the sum of the van der Waals radii (O, 1.4 Å; N, 1.55 Å). [d] The root-mean-squared distance in Å between the minimized TK−**1** and TK−thymidine complexes calculated for all residues within 3 Å of the substrate. [e] The distance in Å between the sugar O5′ and sulfate S atom. [f] The distance in Å between the sugar O3′ and sulfate S atom. [g] The interaction energy in kJ/mol between substrate and enzyme using two different dielectric constants ($\epsilon = 1$ and $\epsilon = r$).

given in Table 1. Very similar results were calculated for all other compounds of Figure 3 (data not shown). As in the case of thymidine, more than 80% of the total binding energy can be attributed to the sugar and nucleobase moieties. Strong hydrogen bonds between the sugar hydroxyls and residues Glu-83, Glu-225, and Tyr-101 and between the amide atoms N3 and O4 of the nucleobase and Gln-125, as well as base-stacking interactions, are responsible for this tight binding.

It is clear that substitution of the 5-methyl group of thymidine by a bulkier, unsaturated group such as a thiophene in **1** has no significant effect on the major binding interactions involving base and sugar moieties. Docking of 5-substituted 2′-deoxyuridine substrates in a conformation which resembles binding mode **1a** positions the 5-substituted group of the substrates in a small pocket where the 5-methyl group of thymidine is also bound. The major fraction of the solvent-accessible surface of this pocket is formed by Tyr-132. A molecular graphics exercise shows that only a small displacement of Tyr-132 is needed to enlarge this pocket such that it becomes large enough to occupy 5-substituted groups like thienyl moieties (Figure 7).

**Understanding the Differences in Affinity of 5-Substituted 2′-Deoxyuridine Substrates: The Role of the 5-Substituted Side Chain.** In an attempt to rationalize the observed affinity differences between the different 5-substituted substrates, a binding energy−affinity relationship study was undertaken. The 18 substrates listed in Figure 3 were alternatively docked in the active site of HSV-1 TK[7] in a binding conformation similar to **1a** (Figures 5 and 6), and their orientations were optimized by means of energy minimization techniques. Several energy calculations were performed for each substrate, each of them differing in the applied dielectric constant for calculating electrostatic interactions or in the number of enzyme residues that were allowed to relax. Interaction energies between substrate and enzyme, under the form of nonbonded van der Waals and electrostatic terms, were calculated for each complex and for each experimental setup to provide a measure of the tightness of binding. The results are listed in Table 4.

In order to account for possible differences in hydrophobicity between the compounds, free energies of solvation for each of the 18 substrates were also calculated. The electrostatic contribution to the total solvation free energy was calculated by solving the Poisson−Boltzmann equation.[19] The nonpolar component of the total solvation free energy was estimated from the solvent-accessible surface of each molecule.[20,21] It was assumed that the differences in solvation free energy between the 18 compounds could be largely attributed to the different substitution patterns at position 5. Therefore, to make the computations computationally feasible and to eliminate a possible dependency of the calculated solvation energy on the conformation of the sugar moiety, the whole 2′-deoxyuridine moiety was replaced by a methyl group. The results are listed in Table 5.

The correlation coefficients for the least-squares fits between the logarithm of the $IC_{50}$'s and the calculated interaction energies, corrected for differences in hydrophobicity, are listed in Table 6. The best correlation is found for the case where the dielectric constant is treated as a distance-dependent function ($\epsilon = r$) and where only the residues positioned within 3 Å of the substrate were allowed to relax. The least-squares equation for this particular case is given by

$$\ln(IC_{50}) = 0.177IE + \Delta G_{sol}/RT + 51.9, \qquad (1)$$

in which IE stands for interaction energy in kJ/mol, $\Delta G_{sol}$ is the solvation free energy of the substrate in kJ/mol, $RT$ is expressed in kJ/mol, and $IC_{50}$ is expressed in $\mu$M. Figure 8 shows a plot of this equation. It is clear from eq 1 that the affinity for this series of 5-substituted 2′-deoxyuridine substrates can be improved either by increasing the side chain's interaction energy (IE more negative) or by increasing the side chain's hydrophobicity ($\Delta G_{sol}$ more positive).

The interaction energies in eq 1 have been calculated without explicit solvent, using a distance-dependent dielectric and by allowing only part of the enzyme to minimize. It is therefore important to stress that both the slope and intercept of eq 1 have no real physical meaning, although in principle some contributions from, for example, enzyme desolvation, conformational entropy, and steric stress should be present. In principle, the equation could be expanded to include these factors as well. However, we have chosen not to do so, mainly

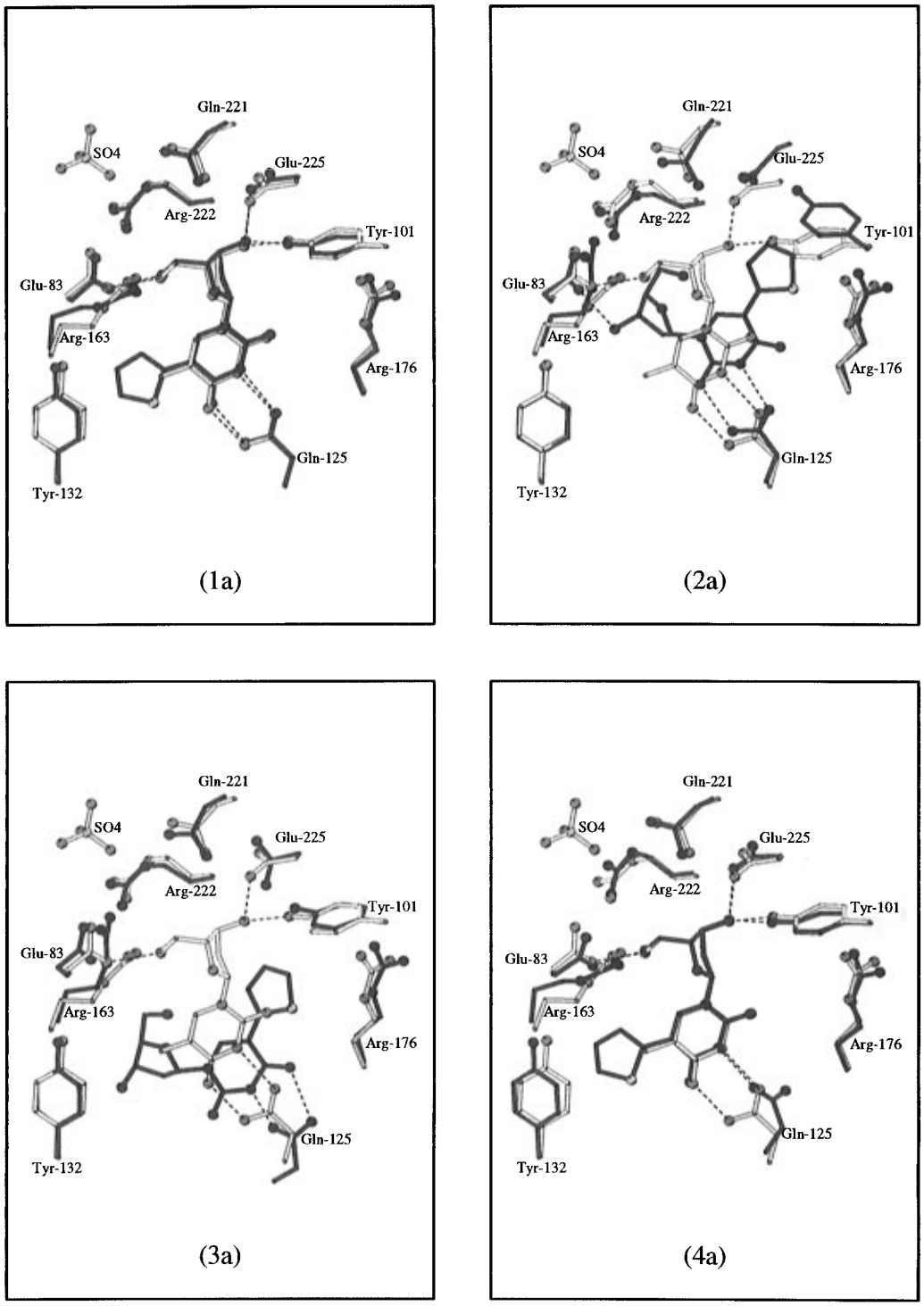


**Figure 6.** 5-(Thien-2-yl)-2′-deoxyuridine (**1**) energy minimized in the active site of HSV-1 TK. Four of the eight possible binding conformations are shown (**1a**, **2a**, **3a**, **4a**; Figure 5). Several residues lining the active-site pocket are also shown. The energy minimized complex between TK and thymidine (drawn using light-colored bonds) is shown as a reference. The substrate and its corresponding residues are drawn using dark-colored bonds. Hydrogen bonds are displayed as dashed lines.

because of difficulties in accurately estimating them and also because of the limited number of data to fit against.

## Discussion

**The Binding Conformation of 5-Substituted 2′-Deoxyuridine Substrates.** On the basis of an exploration of the conformational space of 5-(thien-2-yl)-2′-deoxyuridine (**1**) in the active site of HSV-1 TK, we have found that the most likely binding conformation of these kind of substrates closely resembles that of thymidine (binding conformation **1a**, Figures 5 and 6). This is in accord with the observation that the affinities for the enzyme of many of these 5-substituted 2′-deoxyuridine substrates (Figure 3) are comparable with the corresponding value for thymidine. In this binding conformation the sugar hydroxyl groups are hydrogen bonded to Glu-83, Glu-225, and Tyr-101, and with the pyrimidine base stacked between Met-128 and Tyr-172, and hydrogen bonded to Gln-125. Together, these interactions represent more than 80% of the total interaction energy

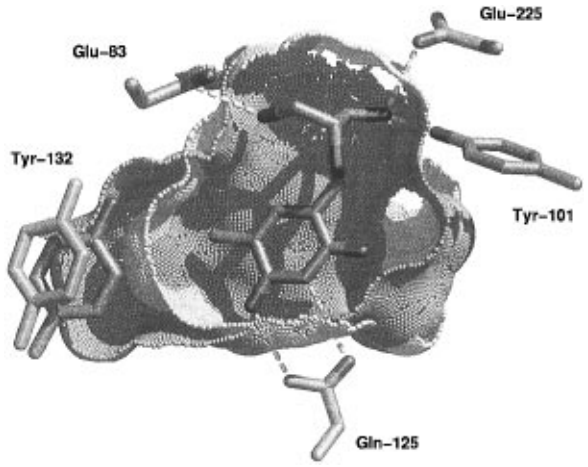


**Figure 7.** Only a minor small position shift of Tyr-132 is needed to enlarge the pocket of the 5-methyl group of thymidine so that it becomes large enough to occupy furane or thiophene groups. The yellow-colored part is the bottom part of the solvent-accessible surface of the pocket as found in the crystal structure, colored in blue is the new pocket after a small position shift of Tyr-132.

**Table 4.** Calculated Interaction Energies (kJ/mol) between Substrate and HSV-1 TK Enzyme

| | residue cutoff[a] | | | | | |
|---|---|---|---|---|---|---|
| substrate | 0 Å | 2 Å | 3 Å | 4 Å | 6 Å | 8 Å |
| | Constant Dielectric $\epsilon = 1$ | | | | | |
| T | −235 | −263 | −285 | −291 | −273 | −265 |
| **1** | −196 | −215 | −309 | −321 | −313 | −316 |
| **2** | −126 | −160 | −281 | −315 | −325 | −328 |
| **3** | −97 | −171 | −256 | −298 | −303 | −307 |
| **4** | −206 | −238 | −282 | −296 | −288 | −296 |
| **5** | −155 | −180 | −297 | −320 | −322 | −325 |
| **6** | −175 | −196 | −299 | −322 | −316 | −325 |
| **7** | −239 | −251 | −299 | −307 | −307 | −309 |
| **8** | −165 | −188 | −292 | −307 | −302 | −305 |
| **9** | −173 | −207 | −274 | −280 | −272 | −275 |
| **10** | −205 | −221 | −312 | −319 | −297 | −306 |
| **11** | −68 | −128 | −272 | −280 | −268 | −278 |
| **12** | −136 | −147 | −281 | −290 | −275 | −282 |
| **13** | −246 | −256 | −307 | −309 | −301 | −304 |
| **14** | −249 | −262 | −316 | −319 | −308 | −306 |
| **15** | −171 | −195 | −291 | −322 | −317 | −320 |
| **16** | −203 | −216 | −290 | −310 | −306 | −301 |
| **17** | −226 | −237 | −282 | −294 | −270 | −269 |
| | Distance-Dependent Dielectric $\epsilon = r$ | | | | | |
| T | −228 | −261 | −285 | −285 | −289 | −283 |
| **1** | −195 | −211 | −305 | −315 | −318 | −311 |
| **2** | −132 | −165 | −272 | −312 | −327 | −325 |
| **3** | −96 | −187 | −259 | −292 | −305 | −299 |
| **4** | −203 | −245 | −279 | −289 | −291 | −286 |
| **5** | −164 | −186 | −293 | −314 | −321 | −322 |
| **6** | −179 | −198 | −292 | −310 | −314 | −314 |
| **7** | −240 | −250 | −301 | −311 | −314 | −309 |
| **8** | −171 | −192 | −294 | −309 | −314 | −306 |
| **9** | −183 | −217 | −265 | −282 | −285 | −288 |
| **10** | −201 | −216 | −308 | −315 | −310 | −310 |
| **11** | −72 | −140 | −267 | −284 | −288 | −282 |
| **12** | −141 | −153 | −279 | −292 | −295 | −289 |
| **13** | −245 | −257 | −306 | −311 | −313 | −305 |
| **14** | −245 | −264 | −312 | −318 | −317 | −312 |
| **15** | −175 | −194 | −288 | −321 | −326 | −324 |
| **16** | −200 | −212 | −283 | −307 | −314 | −313 |
| **17** | −230 | −240 | −287 | −304 | −301 | −296 |

[a] All residues having at least one atom positioned within the cutoff distance of the substrate were allowed to relax. All other residues were kept constrained to their crystal structure coordinates using a harmonic force constant of 1000 kJ/mol·Å$^2$.

(Table 1), and it is therefore anticipated that an alternative binding arrangement lacking one of these

**Table 5.** Calculated Solvation Free Energies $\Delta G_{sol}$ for Each of the 18 Compounds[a]

| molecule | $\Delta G_{np}$[a] | $\Delta G_{ele}$ | $\Delta G_{sol}$ |
|---|---|---|---|
| Me−$CH_3$ | 7.6 | 0.0 | 7.6 |
| Me−1 | 9.7 | −13.9 | −4.2 |
| Me−2 | 10.9 | −9.7 | 1.3 |
| Me−3 | 11.8 | −5.0 | 6.7 |
| Me−4 | 10.5 | −10.5 | 0.0 |
| Me−5 | 10.5 | −10.9 | −0.4 |
| Me−6 | 10.5 | −11.3 | −0.8 |
| Me−7 | 9.7 | −21.0 | −11.3 |
| Me−8 | 9.7 | −16.8 | −6.7 |
| Me−9 | 10.9 | −11.8 | −0.8 |
| Me−10 | 9.2 | −15.5 | −6.3 |
| Me−11 | 10.5 | −10.5 | 0.0 |
| Me−12 | 10.0 | −10.9 | −0.8 |
| Me−13 | 9.2 | −15.5 | −6.3 |
| Me−14 | 9.2 | −29.4 | −20.2 |
| Me−15 | 10.0 | −20.6 | −10.5 |
| Me−16 | 10.0 | −8.4 | 1.6 |
| Me−17 | 9.2 | −7.1 | 2.1 |

[a] $\Delta G_{np}$, $\Delta G_{ele}$, and $\Delta G_{sol}$ stands for nonpolar, electric, and total solvation free energy, respectively. Values are in kJ/mol. [b] Calculated from the solvent-accessible surface area (SAS) using $\Delta G_{np} = 4.7 + 0.046 \cdot (SAS)$. SAS in Å$^2$ and $\Delta G_{np}$ in kJ/mol.

**Table 6.** Correlation Coefficients $r^2$ for the Least-Squares Fits between the Logarithm of the $IC_{50}$'s and the Calculated Interaction Energies, with the Inclusion of Corrections for Differences in Hydrophobicity between the Compounds

| | 0 Å | 2 Å | 3 Å | 4 Å | 6 Å | 8 Å |
|---|---|---|---|---|---|---|
| $\epsilon = 1$ | 0.3 | 0.2 | 0.7 | 0.3 | 0.1 | 0.1 |
| $\epsilon = r$ | 0.4 | 0.2 | 0.8 | 0.6 | 0.3 | 0.2 |

interactions may result in a significantly decreased affinity, as is the case for, for example, acyclovir.[17]

**The Role of the 5-Substituted Heterocyclic Group in Fine-Tuning the Affinity.** The 5-substituted 2′-deoxyuridine analogues differ from the natural substrate thymidine only by the different substitution pattern at the 5-position. The spread in affinity of these compounds is narrow and ranges from 0.3 to 143 $\mu$M (Figure 3). It is likely that these small differences in affinity are the result of structural differences of the 5-substituted groups, and not from different binding conformations of the base or sugar moiety. Any structural changes with respect to these moieties would result in a much more drastic change in affinity, such as in the case of acyclovir which has an $IC_{50}$ of more than 500 $\mu$M compared to 1 $\mu$M of thymidine.[17]

Equation 1 shows that, for this series of compounds, affinity for the enzyme is affected by both the hydrophobicity of the 5-substituted side chain and its interaction energy with the enzyme. According to this model, strong affinity results from the binding of hydrophobic compounds which are also characterized by their ability to interact strongly with the enzyme. Therefore, from the viewpoint of structure-based drug design, it may be of interest to investigate which geometric or electronic factors do influence either the interaction energies of the 5-substituted substrates or their hydrophobicities.

**(A) Factors Influencing the Interaction Energy. (i) Steric Complementarity with the Active-Site Pocket.** A general observation is that the interaction energy between substrate and enzyme decreases as the size of the thienyl of furanyl substituent increases (Table 4, distance dependent dielectric with 3 Å residue cutoff). Comparing, for example, the 2-thienyl ana-

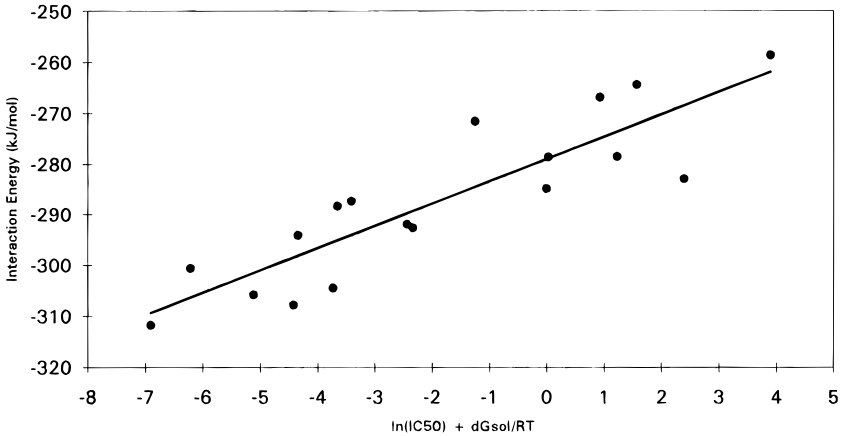


**Figure 8.** A plot of $\ln(IC_{50}) + \Delta G_{sol}/RT$ *vs* interaction energy.

logues, it is clear that the smaller, unsubstituted heterocyclic thiophene ring **1** fits the active-site pocket better than the larger, bromo-substituted thienyl compounds **2**−**4**. The same can be said for the substrates in the 2-furanyl series (**10** > **12** > **11**), or for the isoxazolyl series of compounds (**14** > **15**). Therefore, 5-substituted heterocyclic ring systems with small or no substitutions are preferred in terms of favorable interaction energy.

**(ii) Electrostatic Complementarity with the Active-Site Pocket.** The interaction energy of isoxazolyl **14** or furanyl derivative **10** is more favorable than the corresponding value of thiophene compound **1**. Figure 9 compares the predicted binding conformation of compound **14** with that of **1**. From this figure it can be seen that in the case of the isoxazole ring **14** a stabilizing interaction is formed due to the location of the two electronegative atoms O1 and N2 in a region of positive electrostatic potential. In the case of the thiophene ring **1**, this stabilizing interaction is clearly absent because of the lack of any electronegative atoms in this region of positive potential. Thus, the introduction of electronegative atoms in the heterocyclic ring system at a position that allows them to interact with the positive potential at the back of the pocket may stabilize the interaction between substrate and enzyme to a certain extent.

**(B) The Counterbalance between Hydrophobicity and Interaction Energy.** In the case of 5-substituted 2′-deoxyuridine nucleosides, improved binding affinity for the enzyme can be obtained by ameliorating the compound's hydrophobicity by introducing halogen or methyl groups. However, the introduction of large groups onto the heterocyclic system often leads to a decrease in interaction energy with the enzyme. This in turn translates into decreased affinity so that the final affinity will remain somewhat unaffected. For example, Figure 3 shows there is no remarkable difference in measured affinity between the thiophene substrate **1** and its 2-methyl, 2-chlorine, or 2-bromine analogues (**6**, **5**, or **2**, respectively). However, introduction of a chlorine **12** or bromine atom **11** onto a furanyl ring **10** leads to a decrease in affinity of at least 1 order of magnitude. This is because the gain in affinity due to improved hydrophobicity of **11** and **12** is counterbalanced to a much larger extent by the loss of affinity due to the significant decrease in interaction energy as a consequence of steric clashes between the side chain of Arg-163 and the halogen substituent.

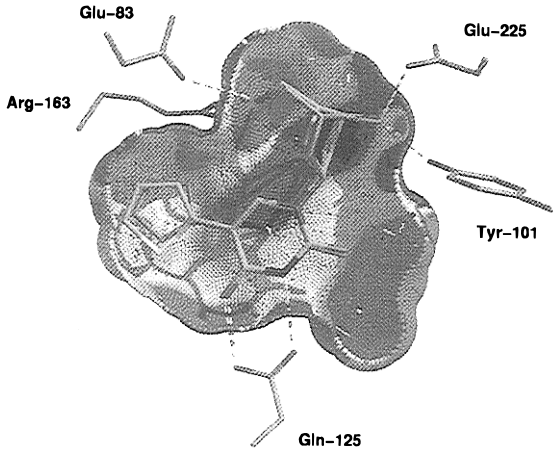


**Figure 9.** The electrostatic potential at the solvent-accessible surface of the active-site pocket. Red is positive potential; blue is negative. The C atoms of the isoxazole compound **19** are colored gray, and the thiophene analogue carbons **1** are colored cyan.

A similar conclusion can be drawn about the introduction of electronegative atoms in the five-membered ring systems. Although the replacement of ring carbons with electronegative atoms often improves the interaction energy due to the favorable interaction with the positive electrostatic potential near the back of the pocket, the resulting structures are characterized by a decreased hydrophobicity. This is exemplified by comparing the affinities of the 2-furanyl substrate **10** with those the isoxazolyl compound **14**. The small gain in affinity due to the increased interaction energy of **14** compared to that of **10**, is completely counterbalanced by the significant loss of hydrophobicity of **14** compared to that of **10**.

It is clear that structural changes aimed at improving the 5-substituent's hydrophobicity are often counterbalanced by decreased interaction energies and *vice versa*. Therefore, for the design of improved 5-substituted 2′-deoxyuridine analogues, it is the drug designer's challenge to search for that molecule which forms the best compromise between hydrophobicity and structural complementarity to the enzyme.

**Validating the Model.** In order to assess the significance of the above derived correlation between interaction energy, hydrophobicity, and affinity (eq 1), its success in predicting the $IC_{50}$ of 5-(pyrrol-1-yl)-2′-deoxyuridine (**18**) (Figure 10) was investigated. This

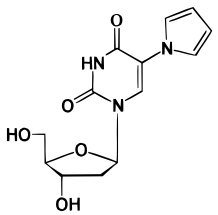

**Figure 10.** The structure of 5-(pyrrol-1yl)-2′-deoxyuridine (**18**) used to validate the derived correlation between interaction energy, hydrophobicity, and affinity.

compound had already been synthesized before, but its affinity for HSV-1 TK had never been measured so far. 5-(Pyrrol-1-yl)-2′-deoxyuridine (**18**) was considered to be a suitable candidate because of its structural resemblance with compounds like those of Figure 3. A total solvation free energy for 1-methylpyrrole of −9.1 kJ/mol and, after docking compound **18** in the active site of HSV-1 TK, an interaction energy of −304 kJ/mol were calculated. Following eq 1, this corresponds to a predicted $IC_{50}$ of 6 $\mu$M, which is in excellent agreement with a measured value of 7 $\mu$M.

## Conclusion

Thymidine kinase from HSV-1 is a key enzyme in the metabolic activation of antiviral nucleosides. High affinity of these compounds for the enzyme is required for efficient phosphorylation. Recently, a new series of 5-substituted 2′-deoxyuridine nucleoside substrates as anti-HSV-1 agents has been discovered, and many of these compounds show high affinity for the viral TK enzyme. The availability of these data in combination with the recently solved structure of HSV-1 TK was an attractive opportunity to investigate the structural factors which would influence the affinity of these compounds for the enzyme.

Modeling calculations indicated that the binding energetics of thymidine and 5-substituted 2′-deoxyuridine analogues are very similar. The majority of the binding energy arises from hydrogen-bonding interactions involving sugar and base moieties. Stacking interactions of the uracil base contribute the remaining binding forces.

Calculations also indicated that the observed affinity differences of the 5-substituted nucleosides are fine-tuned by either the hydrophobicity of the 5-substituted side chain or its interaction energy with the enzyme. Hydrophobicity can be decreased by the introduction of halogen substitutents, whereas the interaction energy can be improved by the introduction of electronegative atoms at well-defined positions, or by keeping the geometry of the five-membered heterocycle small. However, for this series of 5-substituted nucleosides, structural modifications aimed at improving the compound's hydrophobicity are often counterbalanced by decreased interaction energies, and *vice versa*, which makes the design of potent 5-substituted substrates an interesting challenge. The present study also explains why 5-(bromovinyl)-2′-deoxyuridine is one of the strongest binding compounds, and it, finally, gives a qualitative explanation for the first metabolic step in the activation of these class of compounds.

## Experimental Section

**The HSV-1 TK Crystal Structure.** The crystal structure of HSV-1 TK in complex with thymidine was used as starting structure.[7] All crystallographic waters were removed. HBPLUS[25] was used to provide an analysis of the hydrogen-bonding pattern around the Asn, Gln, and His side chains and if necessary to exchange their N/O atoms where the hydrogen-bonding pattern suggested it. Hydrogen atoms were added at geometrically reasonable positions using MacroModel.[26] Polar hydrogens of Ser, Tyr, and Thr residues were repositioned manually based on geometrical and hydrogen-bonding criteria. All His residues were assumed to be neutral. Geometrical and hydrogen-bonding criteria were used to decide between the two tautomeric configurations. Three His residues were modeled with their N$\epsilon$ atom protonated (58, 142, 213), and the other five His residues were protonated at N$\delta$ (105, 164, 283, 323, and 351).

**Charge and Force Field Parameter Development.** The AMBER* force field[24] was used. Partial atomic charges for the substrates were calculated using the standard procedure of fitting the electrostatic potential at the STO-3G level of theory.[29] With the exception of torsion angle and some bond and angle parameters, all necessary parameters for the substrates were provided by the AMBER* force field. Missing bond and angle parameters were derived from comparison with the crystal structures, while their force constants were taken from comparable bonds or angles from the AMBER* force field. In cases where no torsion parameters were available, appropriate parameters were derived by comparison with torsion profiles calculated at the 6-31G* level of theory. However, because we were interested not in molecular dynamics but only in energy minimization calculations, little or no attempts were made to accurately model the height of barrier between local energy minima. A modified AMBER* force field file in MacroModel format containing partial charges and modified force field can be obtained from the authors upon request.

**Energy Calculations.** Energy calculations on enzyme−substrate complexes were performed using the BatchMin module of MacroModel 5.0.[26] No explicit waters or other approaches to model solvent were used because the substrates in the active-site pocket are totally shielded from bulk solvent. Furthermore, nearly all solvent-accessible residues were kept constrained to their crystal coordinates (see further), so that possible conformational changes due to the absence of solvent during the calculations were avoided. After the substrates were docked in the active site, the whole complex was energy minimized until the energy gradient dropped below 0.01 kJ/mol·Å. Other minimization protocols, such as simulated annealing procedures by which the systems were slowly cooled from 300 to 10 K over a 300 ps time scale, followed by energy minimization, did not improve the results to any extent (data not shown). Similarly, medium temperature molecular dynamics in conjunction with energy minimization to explore conformational space did not yield new binding conformations.[30] Either a distance-dependent or a constant dielectric was used to calculate electrostatic interactions using a nonbonded cutoff distance of 10 Å. Only part of the enzyme was allowed to relax, and residues further than a specified distance (0, 2, 3, 4, 6, or 8 Å) from the substrate were kept constrained to their crystallographic positions using a harmonic force constant of 1000 kJ/mol·Å$^2$.

**Calculation of Solvation Free Energies.** The electrostatic component of the total solvation free energy was calculated by solving the Poisson−Boltzmann equation[19] using a finite difference method as implemented by the DelPhi program.[20,22,23] The solvent-accessible surface was calculated with the DMS program of MidasPlus[27] using a probe radius of 1.4 and 0 Å for the solvent calculations ($\epsilon = 80$) and vacuum ($\epsilon = 2$) calculations, respectively. Partial atomic charges were obtained from 6-31G** calculations using the CHELPG procedure of GAMESS.[31] The reduced radii set of Sitkoff and coworkers was used for the atomic radii to calculate the solvent-accessible surface.[20] This procedure should guaranty the calculation of solvation energies with an average accuracy better than 3 kJ/mol.[20] Other charge sets, such as the STO-3G-derived atomic partial charges of the AMBER* force field, were also tried but yielded much less satisfying correlations (data not shown).

The nonpolar component of the total solvation free energy was estimated from the solvent-accessible surface area using standard Pauling radii. A linear least-squares relationship between the nonpolar component of the total solvation free energy and the solvent-accessible surface area was calculated from experimental alkane transfer free energies,[22] and this least-squares relation served to extrapolate the nonpolar solvation energies of the compounds under study.

**Acknowledgment.** Authors are indebted to all colleagues which contributed to this article by their skillful execution of all chemical, physical, biological, and biochemical experiments. Substrates were synthesized in our laboratory by P. Wigerinck, C. Pannecouque, I. Luyten, Liu Jie, A. Van Aerschot, and L. Kerremans. Antiviral data and HSV-1 TK affinities were measured by E. De Clercq and J. Balzarini at the Rega-institute of Leuven, Belgium. Small molecule crystal data were obtained from A. Olivier, C. Evrard, I. Creuven, and F. Durant at the University of Namur, Belgium.

## References

(1) Prusoff, W. H. Synthesis and biological activity of iododeoxyuridine, an analog of thymidine. *Biochim. Biophys. Acta* **1959**, *32*, 295−296.
(2) Herdewijn, P. A. M. M. 5-Substituted-2′-deoxyuridines as anti-HSV-1 agents: synthesis and structure activity relationship. *Antiviral Chem. Chemother.* **1994**, *5*, 131−146.
(3) De Clercq, E.; Descamps, J.; De Somer, P.; Barr, P. J.; Jones, A. S.; Walker, R. T. (*E*)-5-(2-Bromovinyl)-2′-deoxyuridine: a potent and selective anti-herpes agent. *Proc. Natl. Acad. Sci. U.S.A.* **1979**, *76*, 2947−2951.
(4) Spadari, S.; Maga, G.; Focher, F.; Ciarrocchi, G.; Manservigi, R.; Arcamone, F.; Capobianco, M.; Carcuro, A.; Colonna, F.; Iotti, S; Garbesi, A. L-Thymidine is phosphorylated by herpes simplex virus type 1 thymidine kinase and inhibits viral growth. *J. Med. Chem.* **1992**, *35*, 4214−4220.
(5) Coen, D. M. The implications of resistance to antiviral agents for herpes virus drug targets and drug therapy. *Antiviral Res.* **1991**, *15*, 287−300.
(6) Coen, D. M.; Kosz-Vnenchak, M.; Jacobson, J. G.; Leib, D. A.; Bogard, C. L.; Schaffer, P. A.; Tyler, K. L.; Knipe, D. M. Thymidine kinase-negative herpes simplex virus mutants establish latency in mouse trigeminal ganglia but do not reactivate. *Proc. Natl. Acad. Sci. U.S.A.* **1989**, *86*, 4736−4740.
(7) Brown, D. G.; Visse, R.; Sandhu, G.; Davies, A.; Rizkallah, P. J.; Melitz, C.; Summers, W. C.; Sanderson, M. R. Crystal structures of the thymidine kinase from herpes simplex virus type-I in complex with deoxythymidine and Ganciclovir. *Nature Struct. Biol.* **1995**, *2*, 876−881.
(8) Wigerinck, P.; Pannecouque, C.; Snoeck, R.; Claes, P.; De Clercq, E.; Herdewijn, P. 5-(5-Bromothien-2-yl)-2′-deoxyuridine and 5-(5-chlorothien-2-yl)-2′-deoxyuridine are equipotent to (E)-5-(2-bromovinyl)-2′-deoxyuridine in the inhibition of herpes simplex virus type I replication. *J. Med. Chem.* **1991**, *34*, 2383−2389.
(9) Wigerinck, P.; Snoeck, R.; Claes, P.; De Clercq, E.; Herdewijn, P. Synthesis and antiviral activity of 5-heteroaryl-substituted-2′-deoxyuridines. *J. Med. Chem.* **1991**, *34*, 1767−1772.
(10) Wigerinck, P.; Kerremans, L.; Claes, P.; Snoeck, R.; Maudgal, P.; De Clercq, E.; Herdewijn, P. Synthesis and antiviral activity of 5-(thien-2-yl)-2′-deoxyuridine analogues. *J. Med. Chem.* **1993**, *36*, 538−543.
(11) Olivier, A.; Creuven, I.; Evrard, C.; Evrard, G.; Dory, M.; Van Aerschot, A.; Wigerinck, P.; Herdewijn, P.; Durant, F. Stereoelectronic properties of five anti-HSV-1 2′-deoxynucleosides analogues with heterocyclic substituents in the 5-position: A comparison with BVDU. *Antiviral Res.* **1994**, *24*, 289−304.
(12) Creuven, I.; Evrard, C.; Evrard, G.; Wigerinck, P.; Herdewijn, P.; Durant, F. Relationship between structural properties and affinity for HSV-1 kinase of bromine substituted 5-heteroaromatic 2′-deoxyuridines. *Antiviral Res.* **1996**, *30*, 63−74.
(13) Creuven, I.; Evrard, C.; Evrard, G.; Wigerinck, P.; Herdewijn, P.; Durant, F. Crystal structure of 5-(thien-2-yl)uracil analogues: 5-(5-methylthien-2-yl)-2′-deoxyuridine, 5-(5-chlorothien-2-yl)-2′-deoxyuridine and 5-(5-bromothien-2-yl)-2′-deoxyuridine. *J. Chem. Cryst.*, in press.
(14) Creuven, I.; Lebon, F.; Busson, R.; Herdewijn, P.; Durant, F. Structural study of two 5-heteroaromatic-2′-deoxyuridines and their bromine analogues: theoretical conformational analysis and NMR experiments. Manuscript in preparation.
(15) Luyten, I.; De Winter, H.; Busson, R.; Lescrinier, T.; Creuven, I.; Durant, F.; Balzarini, J.; De Clercq, E.; Herdewijn, P. Synthesis of 5-(isothiazol-5-yl)-2′-deoxyuridine and its interaction with the HSV-1 thymidine kinase. *Helv. Chim. Acta* **1996**, in press.
(16) Parkanyi, L.; Kalman, A.; Czugler, M.; Kovacs, T.; Walker, R. T. A comparison of the conformations adopted by some 5-bromovinyl-2′-deoxyuridines and a correlation with their antiviral properties: an X-ray study. *Nucleic Acids Res.* **1987**, *15*, 4111−4121.
(17) Balzarini, J.; Bohman, C.; De Clercq, E. Differential mechanism of cytostatic effect of (*E*)-5-(2-bromovinyl)-2′-deoxyuridine, 9-(1,3-dihydroxy-2-propoxymethyl)guanine, and other antiherpetic drugs on tumor cells transfected by the thymidine kinase gene of Herpes Simplex virus type 1 or type 2. *J. Biol. Chem.* **1993**, *268*, 6332−6337.
(18) Bohman, C.; Balzarini, J.; Wigerinck, P.; Van Aerschot, A.; Herdewijn, P.; De Clercq, E. Mechanism of cytostatic action of novel 5-(thien-2-yl)- and 5-(furan-2-yl)-substituted pyrimidine nucleoside analogues against tumor cells transfected by the thymidine kinase gene of Herpes Simplex virus. *J. Biol. Chem.* **1994**, *269*, 8036−8043.
(19) Davis, M. E.; McCammon, J. A. Electrostatics in biomolecular structure and dynamics. *Chem. Rev.* **1990**, *90*, 509−521.
(20) Sitkoff, D.; Sharp, K. A.; Honig, B. Accurate calculation of hydration free energies using macroscopic solvent models. *J. Phys. Chem.* **1994**, *98*, 1978−1988.
(21) Ben-Naim, A.; Marcus, Y. Solvation thermodynamics of nonionic solutes. *J. Chem. Phys.* **1984**, *81*, 2016−2027.
(22) Honig, B.; Gilson, M. K. Calculation of the total electrostatic energy of a macromoleular system: solvation energies, binding energies, and conformational analysis. *Proteins* **1988**, *4*, 7−18.
(23) Honig, B.; Sharp, K.; Yang, A.-S. Macroscopic models of aqueous solutions: biological and chemical applications. *J. Phys. Chem.* **1993**, *97*, 1101−1109.
(24) Weiner, S. J.; Kollman, P. A.; Nguyen, D. T.; Case, D. A. An all-atom force field for simulations of proteins and nucleic acids. *J. Comput. Chem.* **1986**, *7*, 230−252.
(25) McDonald, I. K.; Thornton, J. M. Satisfying hydrogen bonding potential in proteins. *J. Mol. Biol.* **1994**, *238*, 777−793.
(26) Mohamadi, F.; Richards, N. G. J.; Guida, W. C.; Liskamp, R.; Lipton, M.; Caufield, C.; Chang, G.; Hendrickson, T.; Still, W. C. MacroModel - An integrated software system for modeling organic and bioorganic molecules using molecular mechanics. *J. Comput. Chem.* **1990**, *11*, 440.
(27) Ferrin, T. E.; Huang, C. C.; Jarvis, L. E.; Langridge, R. The MIDAS display system. *J. Mol. Graph.* **1988**, *6*, 13−27.
(28) Kraulis, P. MOLSCRIPT: a program to produce both detailed and schematic plots of protein structures. *J. Appl. Crystallogr.* **1991**, *24*, 946−950.
(29) Singh, U. C.; Kollman, P. A. An approach to computing electrostatic charges for molecules. *J. Comput. Chem.* **1984**, *5*, 129−145.
(30) De Winter, H. L; von Itzstein, M. Aldose reductase as a target for drug design: molecular modeling calculations on the binding of acyclic sugar substrates to the enzyme. *Biochemistry* **1995**, *34*, 8299−8308.
(31) Schmidt, M. W.; Baldridge, K. K.; Boatz, J. A.; Elbert, S. T.; Gordon, M. S.; Jensen, J. H.; Koseki, S.; Matsunaga, N.; Nguyen, K. A.; Su, S.; Windus, T. L.; Dupuis, M.; Montgomery, J. A. General atomic and molecular electronic structure system. *J. Comput. Chem.* **1993**, *14*, 1347−1363.

JM960278V